Analysis of impurity momentum balance and flows in the SOL by SOLPS-ITER modelling.

E. Sytova[1], I.Senichenkov[1], E. Kaveeva[1], V. Rozhansky[1], I. Veselova[1], S. Voskoboynikov[1], D. Coster[2]

[1] *Peter the Great St.Petersburg Polytechnic University, 195251, Polytechnicheskaya ul., 29, Saint Petersburg, Russia*

[2] *Max-Planck Institut für Plasmaphysik, EURATOM Association, D-85748 Garching, Germany*

Corresponding author mail: elizavetasytova@gmail.com

Understanding the behavior of impurities in the SOL is important because distribution of impurity ions in this region influences their transport to the H-mode pedestal and further to the core [1 and references therein]. In the present paper the modeling of plasma edge is made with the SOLPS-ITER transport code [2] for ASDEX Upgrade tokamak with nitrogen seeding. The distribution of the nitrogen in the SOL and private region (PR) is analyzed.

In the modeling transport coefficients were chosen according to Fig. 1 (a), deuterium fueling was set as $2{\cdot}10^{22}$ atoms/s and nitrogen seeding was $2{\cdot}10^{19}$ atoms/s. Ion temperature and density profiles at the equatorial midplane are presented in Fig. 1 (b), (c); profiles at the divertor targets are presented in Fig. 2 (d) - (f).

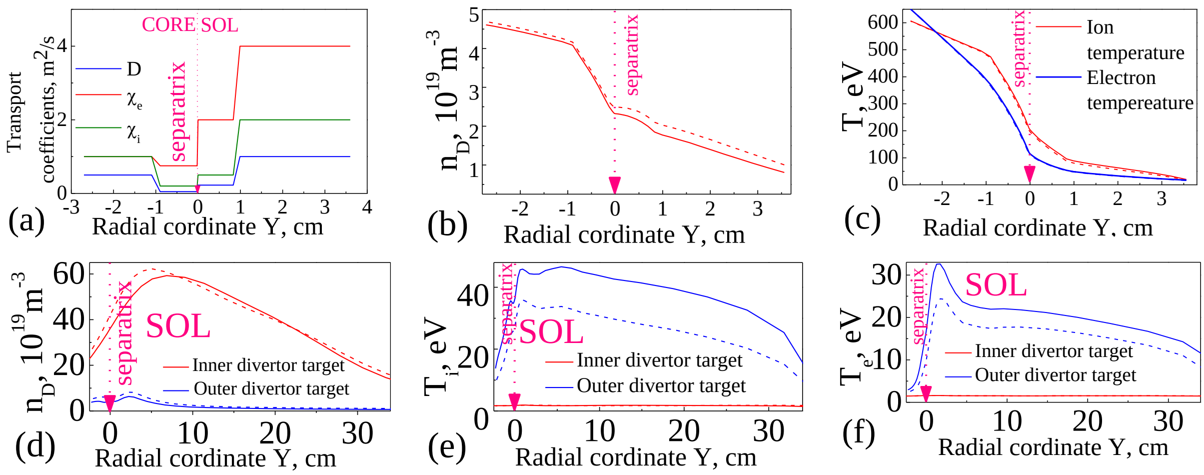

Fig. 1. Transport coefficients (a); radial profiles at the outer midplane of (b) main ion density and (c) temperatures; radial profiles at the targets of (d) main ion density; (e), (f) temperatures. Dashed lines in (b) - (f) correspond to the low pumping case

The distribution of different charged states of nitrogen in the near SOL and in the far SOL is presented in Fig. 2. In the divertor region lower charged states are dominant and in the upper SOL nitrogen mostly exists as N^{+5} - N^{+7} ions.

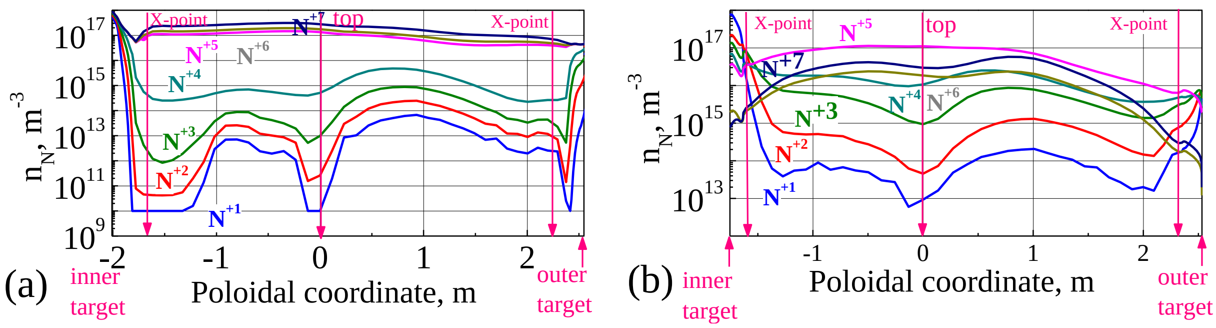

Fig. 2. Poloidal distribution of the nitrogen ions (a) in near SOL (at the distance 1mm from the separatrix traced back to the outer midplane) and (b) in far SOL (16 mm from the separatrix)

To analyze the transport of impurities their parallel momentum balance was observed. One can see that the contribution of forces other than thermal and friction force are small, Fig. 3.

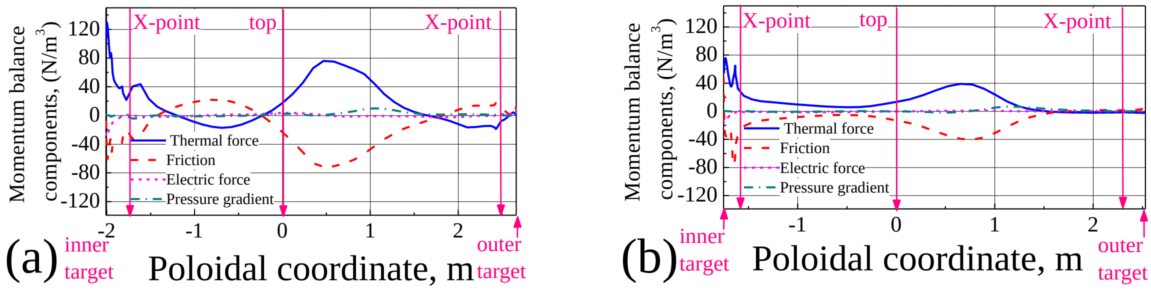

Fig. 3. Parallel momentum balance for nitrogen in SOL (summed over all charged states) (a) in the near SOL (1 mm from the separatrix) and (b) in the far SOL (16 mm from the separatrix)

Therefore, the parallel velocity of nitrogen can be determined from the balance of the friction and thermal force and appears to be a function only of the ion temperature gradient and main ion velocity. Friction force on the impurity ions is $R_{\parallel I} \approx Z^2 n_I n_i m_p \left(V_\parallel - V_{\parallel I}\right)\tau_p^{-1}\sqrt{2}$, and thermal force is $R_\parallel^T \approx 1.56 Z^2 n_I \nabla_\parallel T_i$ (here small contributions from the electron friction and thermal force are excluded), so the parallel velocity of the impurity is $V_{\parallel I} \approx V_\parallel - 1.56 n_i \tau_p m_p^{-1} \nabla_\parallel T_i$. Comparison of poloidal projections of the parallel velocity of nitrogen (averaged over charged states), deuterium, and velocity calculated by the equation above is presented in Fig. 4. In the near SOL the influence of thermal force is significant and nitrogen velocity differs from that of main ions while in the far SOL different plasma species velocities are close to each other.

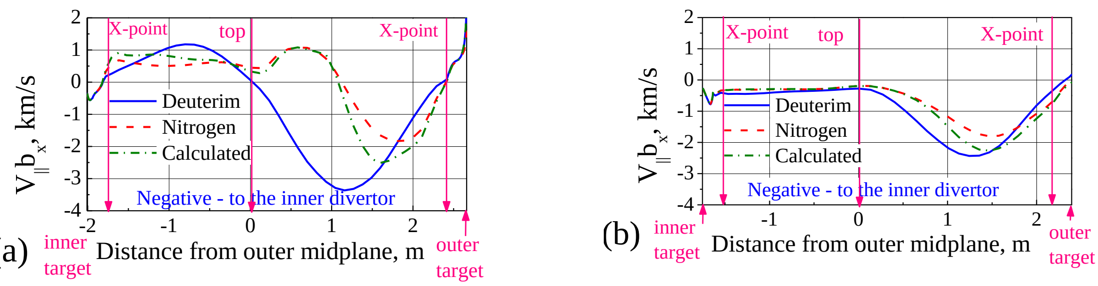

Fig. 4. Poloidal projection of parallel velocities of deuterium ions, nitrogen (averaged over charged states) and calculated in (a) near SOL (1mm from separatrix) and (b) far SOL (16 mm from separatrix)

The global patterns of nitrogen poloidal migration were analyzed using radially integrated flows in the SOL and PR. Poloidal flux of nitrogen outside the separatrix mainly consists of the flux, determined by parallel velocity, and $\vec{E}\times\vec{B}$ flux, Fig. 5. In SOL region the impact of parallel velocity flux is stronger than impact of drift flux, situation in the PR is opposite. It can be noticed, that in both SOL and PR regions nitrogen tends to move towards inner divertor and the flows through SOL and PR are of the same order.

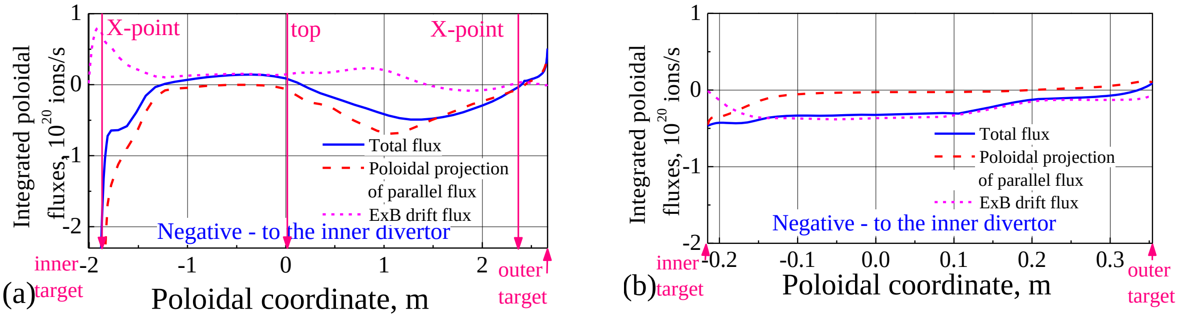

Fig. 5. Poloidal fluxes of nitrogen in SOL (a) and PR (b) integrated radially

Distribution of poloidal velocities of nitrogen in SOL is rather complicated, Fig. 6 (a). In both near and far SOL nitrogen velocity is directed towards the inner divertor, though in near SOL it is mainly determined by $\vec{E}\times\vec{B}$ drift (V_{ExB}) and in far SOL by poloidal projection of parallel velocity ($V_{||}b_x$). In between velocity is determined by the sum of V_{ExB} and $V_{||}b_x$. There are flux surfaces, where the direction of the total velocity changes due to the $\vec{E}\times\vec{B}$ drift towards outer target. Generally, the drifts lead to the mixing of impurity both poloidally and radially between the near SOL and far SOL without pronounced drag to the inner divertor, Fig. 6 (a). In the private region poloidal velocity is determined mainly by V_{ExB} and directed towards inner target.

In the cold inner divertor there is retention of nitrogen almost without any leakage to the upper regions, except for the small volume near the X-point. In the attached outer divertor the nitrogen retention is weak and nitrogen transport depends crucially on the plasma parameters. Nitrogen leakage from the outer divertor region is connected with the thermal force and with the $\vec{E}\times\vec{B}$ drift fluxes which drag nitrogen from the strike point to the X-point and PR. As a result nitrogen concentrates in the inner divertor with much bigger poloidal fluxes and densities of impurity than in the outer divertor, Fig. 6 (b, c). The integrated flow of nitrogen to inner plate is $6.2\cdot10^{20}$ s^{-1} and to outer plate is $0.9\cdot10^{20}$ s^{-1}. The asymmetry for main ions is smaller - integrated flows are $2.2\cdot10^{23}$ s^{-1} for inner target and $1\cdot10^{23}$ s^{-}1 for outer one. The return flow of nitrogen from inner to outer divertor is provided by neutral flux under the dome.

For the case with low pumping and higher density of outer divertor plasma (dashed lines in Fig. 1) lower nitrogen density in upper SOL is observed. The increase of main ion density leads to smaller temperature in the divertor and therefore better retention of particles, both in accordance to model described in [1] (increase of the friction force) and due to decrease of drift velocity. Since the pumping is from the outer divertor, the better retention of impurity there leads to increase of pumping efficiency and to the overall plasma clean-up. For smaller pumping the nitrogen density is smaller in the near SOL and at the same time bigger at the outer divertor strike point, Fig. 6(d). The overall amount of ionized nitrogen in the SOL above X-point is $2.4 \cdot 10^{17}$ for low pumping and $4.4 \cdot 10^{17}$ for high pumping.

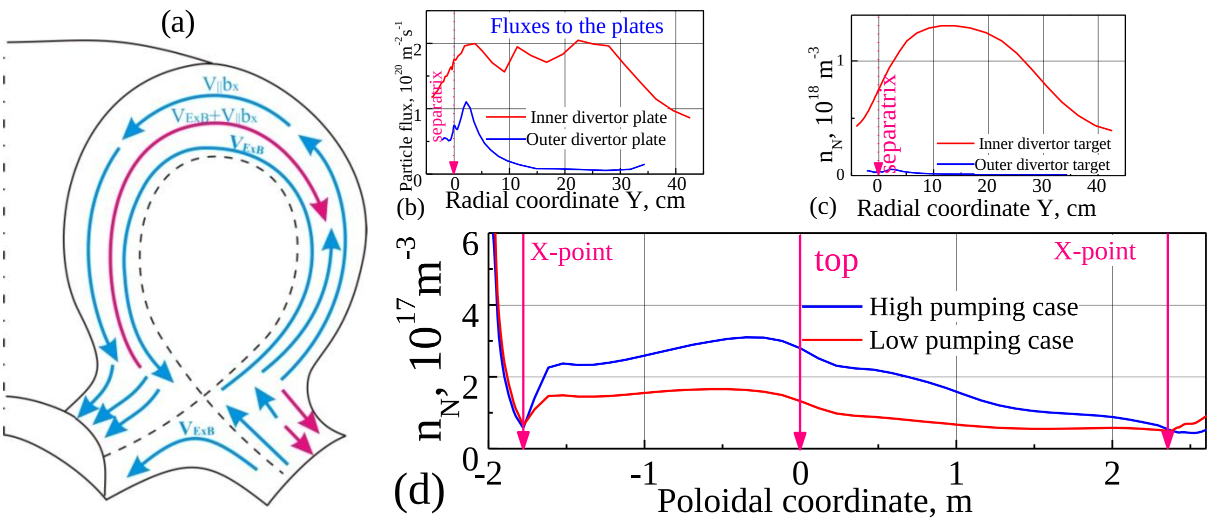

Fig. 6. (a) Sketch of poloidal fluxes of nitrogen in SOL ; (b) distribution of nitrogen poloidal fluxes at the inner and the outer divertor target; (c) distribution of nitrogen density at the inner and outer divertor target; (d) poloidal distribution of the nitrogen density in SOL for low and high pumping

Conclusion.

The transport of nitrogen impurity ions in SOL and PR is analyzed. Distribution of the parallel velocity of nitrogen ions is mainly determined by the balance of friction and thermal force, impact of the $\vec{E} \times \vec{B}$ drift velocities is also significant in the near SOL and in PR. General direction of the ionized nitrogen transport in SOL and PR is towards the inner divertor, where good retention of nitrogen is observed. In the outer divertor region there is a leakage of the nitrogen due to thermal force and drift fluxes impact. The nitrogen flux patterns in SOL and PR are complex and to reproduce them the numerical modeling is necessary.

Acknowledgements

The work was supported by grant of Russian Ministry of Education and Science “Filaments and stochastization”. Authors are also grateful for financial support from the Russian Ministry of Education and Science (Agreement No. 14.619.21.0001, 15.08.2014, id RFMEFI61914X0001).

References

1. Stangeby P. The Plasma Boundary of Magnetic Fusion Devices (ISBN 0750305592)(IoP, 2000)
2. S. Wiesen et al., Journal of Nuclear Materials 463 (2015) 480-484